Stability of rigid motions and coating films in bicomponent flows of immiscible liquids

by Daniel D. Joseph and Luigi Preziosi

Abstract

We consider the problem of global stability of the rigid rotation of two fluids. The realized interfacial configurations minimize a potential. We derive the most general form of the potential in which the working of the contact line may be expressed as a potential. The resulting variational problem for the interfacial potential is solved when the contact line conditions are suppressed and for coating flows in which the interface makes a tangent contact with the wetted rod. In the former case, good agreement with experiments is obtained except near lines of contact. This shows that a spinning rod interfacial tensiometer is viable. In the latter case of coating flow, we get good agreement with experiments when the effects of gravity are not too large. The problem of bifurcation of coating flow is discussed qualitatively and some experimental results are given. We show how bifurcating sequences fit well into our qualitative description of the solution which must minimize the interfacial potential as the angular velocity is increased. The last bifurcations lead to pendant drops on a rotating “ceiling” under the influence of centripetal forces which replace gravity. The dynamics of rollers of oil in water, or part in water and part in air, are explained in terms of the wave length dependence of rotating drops.

1.

Introduction. The problem of placements and the problem of shapes

Flows of two fluids are important and interesting because they are commonplace, they lend themselves to technological applications and they introduce new phenomena without counterpart in the flow of one fluid.

Many configurations of flow of two fluids are possible. We see layers, slugs, rollers, sheets, bubbles, drops and emulsions and foams (see Joseph, Nguyen and Beavers [1984, 1986], hereafter called JNB). These structures are often topologically different from the rest configurations from which they arise. The evolution involves breakup of liquids, a process which is not included in the usual statements governing dynamics (say, the Navier-Stokes equations). In some approximate sense, the configurations and the flow of two fluids which are ultimately achieved in practice are controlled by the problem of placements and the problem of shapes. In the problem of placements, we must describe the massive transport required to position the two fluids in the places they ultimately occupy. This problem is controlled by fingering flows and breakup and frequently is such that the low viscosity constituent is found in the regions of high shear. Some suggestive ideas about the sets of solutions of the problem of placements which may be realized in practice can be determined by arranging the liquids to minimize the dissipation. Actually different minimum problems can be imagined (see JNB) and probably none of them are precise statements of what dynamics will allow. It may in fact be more useful to express the type of "minimization" achieved by the fluids in the anthropomorphic terms used by JNB: "High viscosity liquids hate to work. Low viscosity liquids are the victims of the laziness of high viscosity liquids because they are easy to push around."

The problem of shapes has to do with the geometric form of the interfaces between flowing fluids. This problem involves surface tension and other potential terms which enter into each problem. The problem of shapes for rigid rotations of two fluids was considered by Joseph, Renardy, Renardy and Nguyen [1985], hereafter called JRRN. This paper extends and solves the problem of shapes posed by them.

The problem of placements can be framed as a variational problem for configurations which minimize a dissipation. This variational problem is perhaps a suggestive but not exact statement of the placements allowed by dynamics. The problem of shapes can also be framed as a variational problem. In this problem we seek the shapes which minimize a potential energy. In general this variational problem is also merely suggestive but in some limits it is also exact. The problem of rigid rotations of two fluids without gravity is one of these special cases in which the shape of the interface may be determined by minimizing a potential.

2. Energy theory of stability of rigid motions of two fluids with contact lines

2.1 Steady rigid rotation of two fluids

Rigid motions of a fluid are possible provided that the fluid rotates steadily about a fixed axis. Drops, bubbles, different types of fluids in all types of containers may rotate rigidly. Various kinds of perturbations of rigid motion are also of interest.

A single liquid which fills a container rotating steadily around some fixed axis will eventually rotate with the container. But in the case of two fluids it is necessary to determine the places occupied by the two fluids and the shape of the interfaces between the two fluids.

We shall consider the special case in which the two liquids occupy the region

(Equations 2.1–2.5 and text.)

2.2 Disturbance equations

Set

(Equations 2.6–2.13 and text.)

2.3 Energy equation for rigid motions of two fluids

The disturbance equations given in Section 2.2 imply that

(Equations 2.14–2.19 and text.)

2.4 Assumptions about the interface

We assume that the interface …

We also assume that the boundary …

2.5 Reduction of the interface terms

We proceed now to the terms on the right of (2.17). These were computed by JRRN for the periodic problem and by C. Guillopé and D.D. Joseph for this paper …

(Equations 2.20–2.30 and text.)

2.6 The interface potential

In order to reduce the interface terms (2.30) to potential form we assume that …

(Equations 2.31–2.33 and text.)

Finally we note that the working of the contact line cannot always be represented by a potential. The relation of the assumptions (i) and (ii) which lead to a potential and the classical ones in which contact angles or contact lines are fixed is obscure. We note, however, that these assumptions hold trivially for the case of a fixed line or a constant angle independent of position and, in general, whenever implicit relations of the form □ or □ are valid.

2.7 Poincaré's inequality and the energy inequality

(Equations 2.34–2.37 and text.)

2.8 Integrability of the energy

Integrating (2.37) …

(Equation 2.38 and text.)

2.9 Minimum of the potential

Let us consider the limit configuration …

(Equations 2.39–2.41 and text.)

2.10 Relation between the contact line and the contact angle

Assumptions (i) and (ii) are equivalent to assuming a functional relation in which the contact angle is determined by its position on the contact line. (We could also state equivalent conditions in which the contact line is determined by the angle; say, the contact line does not move.) Precisely, such a functional relation is a differentiable map …

(Unnumbered equations and text.)

… The contact line moves about 1 cm in 3 days, so that the velocity of the contact line is negligible and the angle does not depend on the velocity.

2.11 Spatially periodic connected interfaces

In this section we shall assume that the interface is a graph

(Equations 2.42–2.43 and text.)

3. Solutions of the minimum problem

3.1 Mathematical formulation of the minimum problem

Joseph, Renardy, Renardy and Nguyen [1985] showed that rigid motions of two liquids between concentric cylinders …

(Equations 3.1–3.10, I, II, and text.)

3.2 Analysis of the minimum problem

(Place Figures 1, 2, and 3 near here.)

It is convenient to replace the parameters …

(Equations 3.11–3.24 and text.)

3.3 Periodic solutions, drops and bubbles

(Place Figure 4 near here.)

Solutions which cross the axis may be regarded as limiting cases of periodic solutions. Then we get a periodic array of drops …

(Unnumbered equations and text.)

3.4 All the solutions with J<4 touch the cylinder

Minimizing solutions which cross the axis of rotation will certainly touch the inner cylinder. The prediction that solutions with J<4 will touch the cylinder is completely consistent with experiments. The cylinder touching solutions which are observed are of two types: (i) The interface between the two fluids intersects the cylinder at lines of contact, as shown in Figs. 5, 6, and 13 and (ii) The interface between the two fluids makes a tangent contact with the wetted rod at r=a as shown in Figs. 7 through 11. The physical mechanisms embodied in the difference between (i) and (ii) are associated with fundamental problems of adhesion and cohesion not considered here.

The effects of capillarity at lines of contact should be considered for solutions of type (i), as in (3.23); but if □ is small, the effects of capillarity at contact lines will then also be small. The comparison between theory and experiment shown in Section 5.1 shows that contact line effects are local even in cases when the interfacial tension is large; say when a is small compared to the bubble radius. In the other case (ii), with tangent contact, and no contact line, we acknowledge a constraint on our variational problem, by looking for periodic solutions with troughs which touch the cylinder at r=a. This also works well (see Fig. 7 through 11).

3.5 Critical remarks about stability theory

The fact that realized solutions with J<4 touch the cylinder are a motivation for remarks which are meant to be critical of current ideas about the study of stability of the flow of two fluids. When there is one fluid, there is a unique stable flow at low Reynolds numbers. When there are two fluids, there can be many configurations, even at zero Reynolds numbers. In the case of rigid motions, heavy fluid outside or inside and even nested sequences of drops and bubbles are possible. Different solutions can be realized in nature. So we have not got a unique solution to study but perhaps an infinity of such solutions (see JNB for examples). If we choose one of these and show instability, we eliminate one placement, but we have to study all the others. So with two fluids the identification of a basic flow and the study of its stability cannot be separated.

As an example of the considerations just discussed we note that C. S. Yih [1960] studied the problem of stability of a film of liquid rotating in air. He treats this problem in the linearized approximation. He studies the stability of rigid motions with a free surface of constant radius with gravity neglected. Naturally these constant radius interfaces are unstable because J is negative. Rigid motions, with negligible gravity, are stable and can be obtained easily in experiments (see Sections 5.3 and 5.4) but the free surface cannot have a constant radius.

4. Experiments with heavy fluid outside—the spinning rod tensiometer

(Place figures 5 and 6 near here.)

The case J>0 corresponds to centrifuging, with heavy fluid outside, and 0<J<4 is the domain corresponding to rigid rotation of bubbles whose long dimension increases monotonically from that corresponding to a sphere at …

(4.1)

for values of □ such that gravity is negligible.

The spinning rod tensiometer (U.S. Patent 4,644,782) is a device for measuring interfacial tension between different liquids. This device competes with various spinning drop tensiometers (see Rosenthal [1962], Princen, Zia and Mason [1967]). The rod and the drop tensiometers are designed to work under conditions of negligible gravity in which (2.4) and (4.1) hold simultaeously.

The working formula □ for the spinning rod tensiometer may be replaced with the working formula □ for the spinning drop tensiometer when

(unnumbered equation)

where □. We may ignore the rod when a is small, □ is large of the contact angle at the rod is near to the angle on the bubble without the rod at the same radius.

The shape of rotating bubbles does not depend on whether a small rotating rod pierces the central axis of the bubble, except near lines of contact. This lack of sensitivity of shape on rod is partially controllable, the capillarity is reduced in small rods and may be reduced by using rods of different material and coated rods.

The experimental apparatus used to obtain the results reported here is a cylindrical container of plexiglass with inner radius 3.6 cm., of length 24.5 cm., closed at each end. A rod may be inserted along the central axis. The rods are attached rigidly to the cylinder and all the parts rotate together as a rigid body. We used aluminum rods of radius 0.24 cm. and 0.5 cm. and a plexiglass rod of radius 1.25 cm. A photograph of the cylindrical interface which appears whenever J>4, shown as Fig. 4, will aid the reader in visualizing the cylinder apparatus.

The liquids used in our experiments were water, Castor oil, Soybean oil and 20, 1000 and 12500 cp silicone oils. The densities of these liquids are 1, 0.960, 0.922, 0.949, 0.967, 0.975, respectively. The small density difference greatly reduces perturbing effects due to gravity. The effects of gravity can be reduced to negligible levels with |J|<4 when the density differences are <0.1 and d<1 cm., as in our experiments. If we suppose that □ for k >> 1, then (4.1) requires that □. Under these conditions we always get centrifuged configuration with heavy fluid outside, □.

Solutions of permanent form, periodic in x, with heavy fluid outside (0<J<4), were never observed. Instead of periodic solutions we found isolated bubbles of light liquid centered on the rod. When J>4, we get a cylindrical interface which is modified by capillarity at the end walls. The effects of capillarity are smaller when J–4>0 is larger. When J is reduced from above to below 4, the interface deforms continuously until points at the interior touch the axis. At this point we see some changes in the topology of the interface. The fluid may rupture into bubbles separated from the heavy liquid outside by well defined contact lines. This depends on energetic considerations associated with the two fluids and the rod. The configuration of permanent form which we see most frequently when 0<J<4 is like that shown in Fig. 5 in which small bubbles and large bubbles both appear.

We define d for an isolated bubble as the radius associated with a right circular cylinder of the same length and volume. It follows that there are different J's for small and large bubbles rotating with the same □. This is why the small bubbles are almost spherical and the large ones are elongated.

Agreement between theory and experiment is demonstrated in Fig. 6. The dots represent theory with capillarity neglected. The value of the interfacial tension may be selected to make theory and experiment agree for one value of □. The same interfacial

tension then gives agreement for other values of □. In Figs. 6a and 6b we can compare the agreement between theory and experiment for two different values of □, with one T. Figs. 6a through 6c show that capillarity is a small effect. This was true for all the cases we studied. Figs. 6c and 6d exhibit a worse case situation, comparing a free bubble to a captured bubble, using the same interfacial tension, which is not at all bad.

Very rapid measurements of surface tension may be obtained using elongated bubbles with aspect ratios greater than 6 by assuming that J ⁄ 4. More detailed comparison of theory with observed shapes leads to values of the interfacial tension T.

Some of the advantages enjoyed by the spinning rod tensiometer over various spinning drop tensiometers currently used are (1) the rod captures the bubble eliminating the position problem, (2) the captured bubble is stable if small enough, eliminating the stability problem, (3) the rod reduces the spin-up time from hours to minutes and (4) the cylinder plus rod device is simple and cheap and has a potential for high precision.

5. Experiments with heavy fluid inside—coating flows

We did experiments with heavy fluid outside, “drop” experiments, of a special kind, coating aluminum and plexiglass rods rotating in air with oil. With air outside, □ is not small and gravity can be important. The coating liquids used in our studies were STP, 1000 and 6000 poise silicone oils. The viscosity of STP is about 100 poise. The dynamics which we have observed are not inconsistent with the observations of Moffatt [1977] of films of golden syrup (80 poise) rotating in air. Our study complements Moffatt’s in carefully examining the axial structure of the rotating films as well as the azimuthal variations. We are interested in demonstrating that the shapes of the films are largely determined by minimizing the potential expressing energies associated with centripetal acceleration and surface tension, even when gravity is not negligible.

The apparatus used in these experiments is nearly identical to the one used in the experiments of Moffatt [1977]. A layer of liquid was first coated on the cylinder by rotating it while partially immersed in a trough; the roller was then raised from the trough while still rotating. The coating films achieved in this way could be maintained indefinitely. The films undergo many different transitions as flow parameters are changed. We used 3 different rods: 2 aluminum rods with radius and length 1.02, 30 cm. and 1.42, 45 cm. respectively and 1 plexiglass rod with radius and length 2.04, 30 cm. The material and length of the rods is not important. The liquids coated the entire rod along its whole length.

All the fluids which were mentioned in the last paragraph are sticky. Once the rod is coated with these fluids, it stays coated; dry patches do not develop. This means that contact line conditions are inappropriate for such coating flows. We are then obliged to reconsider the implications of the fact that in unconstrained problems the minimizing

solutions cross the axis when J<4. In the case of sticky coats on rotating rods we have a constrained variational problem in which we require that if the interface touches the rod it will do so with a flat angle of contact at touching points. In fact all the realized solutions touch the rod in just this way (see Figs. 7, 9, 10 and 11).

The same oil which sticks on solids immersed in one fluid need not stick when immersed in another fluid. Silicone oil sticks to plexiglass rods rotated in air, but not in water (see Figs. 12 through 14) even though silicone oil preferentially wets plexiglass.

Some gross features of rod touching oil films rotating in air may be explained as follows. Uniform coats are unstable and undulations begin to develop along the rod. Moffatt [1977] gave a heuristic argument which explains why this instability should not equilibrate until the troughs of the wavy interface touch the cylinder. In this argument we neglect surface tension and suppose that a liquid is rotating in air with □ on □. Then

(unnumbered equation)

and the pressure under any bump is less than the pressure at the side of the bump. In the absence of countervailing forces the pressure deficit would exaggerate the bump, with largest pressure gradients along lines from the point at the base of the bump where □ is minimum. This pressure gradient pulls in the sides of the bump, exaggerating bumpiness. This heuristic argument does not require axisymmetry; it works as well for bumps as for rings. The same argument works without change whenever the heavy fluid is inside, □. When the speeds are low, axisymmetric wavy solutions with troughs that touch the cylinder minimize the interface potential (see Section 5.2). It is nearly impossible to pass fluid from one wave to another. Further increases in the angular velocity lead to increases in the amplitude of the undulations and length of the troughs touching the cylinders. These features are evident in Figs. 7 through 14 of this paper and Figs 5 and 6 of the paper by Moffatt. The undulations are then isolated from one another and not useful to think of periodic (in x) solutions, however periodic they may appear to be. Periodicity can be more closely simulated when the viscosity of the coating fluid is smaller. In this case the transfer of fluid from one undulation to another, which is required to maintain periodicity against disturbances, is enhanced. It may be useful to think of the undulations as rotating drops constrained by tangent contact at the rod. From these explanations the reader should understand why long very thin films separate rotating drops making tangent contact, whether or not the array of drops appears to be periodic.

5.1 Effects of gravity

(Place figures 7 and 8 near here.)

The analysis of Moffatt [1977] and the analysis and experiments of Preziosi and Joseph [1987] show that the effects of gravity on coated rods rotating in air are small when

(Equation 5.1 and text.)

5.2 Computation of the interface shape of rigidly rotating coating flows making tangent contact at the rod

We first determine d in the plane …

5.3 Bifurcation of coating films to non-axisymmetric shapes

The problem of shapes of interfaces between fluids which rotate rigidly without shear, when gravity is neglected, is determined by a balance of the capillary force against pressure forces associated with centripetal accelerations. When there is no rotation, and no other constraints, surface tension will pull the interface into a sphere.

The argument of Section 4 applies equally to axisymmetric shapes (rings) and non-axisymmetric ones (bumps). The stability of rings for small amplitudes and their loss of stability to non-axisymmetric shapes at large amplitudes can be argued from the form of the dimensionless potential.

(Equations 5.2–5.5 and text.)

… modes of azimuthal periodicity.

The bifurcation of axisymmetric figures of equilibrium to first mode, eccentric figures is a robust and possible generic phenomenon, readily observed on nearly every type of coating film, whether rotating in air or in water (see Figs. 9 and 10). The same type of first mode azimuthal periodicity was observed in the [1863] experiments of Plateau (see his Fig. 4) as the first bifurcation of the olive oil drop coating the rotating disk in an alcohol-water mixture. This type of instability does not make sense for free rotating drops since the central axis of a free drop is not fixed in space.

Nonaxisymmetric one-lobed shapes were analyzed by Brown and Scriven [1980] for a drop captured between two rotating disks. These calculations showed that higher lobed shapes between disks, like those reported by Plateau and here are indeed unstable. First mode, eccentric figures, like the shape of drops rotating on a rod, can even be explained within the context of static figures. In his observations of static capillary bridges, Plateau observed such a bifurcation when the end plates confining the neutrally buoyant fluid were brought sufficiently close to one another. This reduces the wave length, as in the case of rotating drops, until the price paid by further decrease of the axial wave length in minimizing the potential is greater than that for bifurcation into

the first mode. Russo and Steen [1986] have recently analyzed this bifurcation in the context of static figures.

5.4 Intrinsically steady and unsteady coating flows

(Place figure 11 near here.)

Flows which are steady in laboratory coordinates can be achieved when □ is small. For larger values of □, these flows are unsteady in every coordinate system. For very large values of □, thin films rotate rigidly and are steady in a rotating coordinate system.

It is impossible to maintain an interface of constant radius on a film of liquid coating a rod rotating in air. If the coat is thick gravity can be very effective in creating a large secondary motion with gravity opposing the motion on one side of the film and supporting it on the other. The effects of gravity are greater when there is more liquid on the rod. For fixed volume of liquid, the effects of gravity are diminished when the viscosity is increased; however, more liquid will remain on the rod at given speed when the liquid is more viscous (cf. Section 4). The two effects compete. At low speeds an equilibrium is established with a “lop-sided” configuration as in Fig. 4b of Preziosi and Joseph [1987] which is steady in laboratory coordinates.

As the speed of rotation is increased the out of roundness begins to increase and also to rotate relative to laboratory coordinates. This is a manifestation of bifurcation to a mode one azimuthal variation, but it is slightly masked by out of roundness due to gravity (see Fig. 9). Such solutions are intrinsically unsteady. At the same time the crest of the waves grow and rings develop, in the manner shown in Fig. 10 and in Figs. 7 and 8 of Moffatt [1977].

When the coating fluid is very viscous and the coating film is thin, the effects of gravity will be diminished, as shown in Fig. 10. Thin films can be created by centrifuging away excess fluid. If the speed of rotation is further increased, more liquid will be flung off the rod. At very high speeds most of the fluid is thrown off the rod. Gravity has nothing to do with “throwing off” because ejected particles of fluid are flung out radially. An equilibrium is reached in which there are pendant drops on a rotating rod. These are shown in Figure 11.

Pendant drops are a symmetry breaking bifurcated solution of our coating film. They tend to form on the rings of earlier solutions with successive rows staggered so that the drops in one row lie in the interstice of the next row. This induces the diamond symmetry shown in the figures. The pendant drops are like those which might develop under gravity on a moist ceiling with an effective gravity equal to □

6. Rollers

(Place figures 12, 13, and 14 near here.)

This section is partly an addendum to the two papers of Joseph, Nguyen, Beavers [1984, 1986] in which we try to explain what is observed there using what we have learned here.

6.1 Rods coated with oil rotating in water, rollers and drops

We are going to discuss two fluid situations in which both fluids do not rotate rigidly. We are interested in situations in which oil coats the rod and both the rod and the attached oil rotate in water. If the oil is sufficiently viscous, it will rotate with the rod as a rigid body. This rigid rotation was achieved in all our experiments with STP, 1000 and 6000 poise silicone oil. We could but do not give the boring data which show that the oil masses rotate rigidly. It is also of interest to consider cases in which the rigid rotating rod plus oil is immersed partly in water and partly in air, as in Fig. 12. The oil bodies which rotate as rigid wheels in fluids of smaller viscosity have been called rollers (see JNB). The dynamical problem posed by the [1863] experiments of Plateau in which olive oil drops on a disk were rotated in an alcohol water mixture also falls in this frame.

We are going to say that oil masses rotating rigidly in water are analogous to drops. This contradicts the static definition of a drop which is when the heavy fluid is inside ($J<0$). Rollers and Plateau's "drops" have the light oil inside ($J>0$). We call these "static bubbles" drops because they act like drops when they are rotated, the length $\square$ along the axis of rotation of these drops or rollers shortens and the maximum radius $\square$ increases as the angular velocity $\square$ is increased. We have not reconciled the obvious difference between the static and dynamic definitions of a drop.

It is necessary to say that the cases under discussion here differ from those in Section 5 in that the water is confined to a stationary box and the water does not rotate rigidly, though the oil does.

Plateau [1863] reports that he observed an unstable toroidal figure of equilibrium, stable for a time, when he increased the rate of rotation of the disk driving the oil drop in the density matched bath of alcohol and water. The sequence seen by him is like that shown in Fig. 3, (b) and (c), a solution of nodoid type valid for rotating drops.

In Fig. 12 we show fat rollers of STP rotating rigidly, lubricated everywhere by water, immersed in water at the bottom and with their tops poking into air. Gravity enters into the dynamics of these rollers; the water pushes up on the bottom and the air pulls down with a much bigger pull at the top. These gravity effects are stabilizing, tending to stabilize otherwise unstable toroidal drops of equilibrium. Fig. 14 of JNB is another even better example of a nodoid type solution of toroidal shape modified by gravity.

Photographs of interpenetrating rollers immersed partly in water and partly in air have been exhibited in JNB [1984, 1986]. The dynamics of these rollers are partly explained by drop dynamics. The first dramatic dynamic event in the formation of

interpenetrating rollers is that a sheet of water fingers through the STP joining the two rotating cylinders, splitting the STP into more or less thick cylindrical films, each on its own cylinder. These films develop the same type of undulations which are charateristic for films rotating in air. The undulations grow in the manner consistent with rotating drops. However their growth is blocked by the presence of the second cylinder and they form square rollers which are consistent with minimizing a drop potential subject to a unilateral constraint.

6.2 Sidewall detachment of single rollers

Sidewall detachment of single rollers was described by JNB and by JRRN. An attempt to describe the underlying dynamics was made by JRRN. They say that the most interesting feature of the dynamics leading to the formation of rollers is the fracturing of the viscous liquid at some critical level of the stress. In this process the roller breaks away from the sidewall and relieves the high stress associated with no slip at the sidewall. So in the final, stable dynamics, rollers are lubricated by water and air on all sides. The rollers rotate nearly as rigid bodies because they are so viscous. The stability of rollers, as our analysis suggests, depends on the fact that the density stratification is such as to prevent the centrifuging of the roller.

Several major points in the foregoing analysis must be revised in the light of our work here. The first revision does away with the notion of a critical stress. The sidewall detachment takes place as a kind of instability associated with a critical angular velocity. Photographs of this instability are exhibited as Fig. 15 of JNB.

We now want to explain sidewall detachment in terms of drop dynamics. The roller will attach to the side wall at all values of □ below a critical one for which the length of the drop with contact at r=a is equal to the distance between the sidewalls. For larger values of □ this length is less than the distance between sidewalls. This line of thought appears to explain qualitatively all of our observations of side wall detachment (see Fig. 13). The foregoing explanation can be made quantitative under the hypothesis that the oil roller completely immersed in water is the same as a roller with an effective density equal to the density of water minus the density of oil, like a light drop rotating in air without gravity. We have not been able to justify this hypothesis mathematically, but it is consistent with the measurements reported in the caption of Fig. 13.

We close this discussion of oil masses rotating in water with some remarks about bifurcation. Again it is necessary to revise JRRN in which it was said, “This instability (to non-axisymmetric disturbances) is associated with viscous shearing, which becomes important at higher speeds and with a possible unstable distribution of angular momentum.” We want to deemphasize the effects of viscous shearing and to emphasize the intrinsic instability. The arguments given in Section 5.3 apply here. In general we get bifurcated sequences in the order of increasing azimuthal periodicity, first n=1 as in Fig. 14(a), then n=2 as in Fig. 14(b). Some higher values of n are shown

in Fig. 14(c) and 14(d). The viscous shearing is very important for the bifurcated figures shown in Fig. 14(c), but it is not the cause of the bifurcation. Our observations of bifurcating sequences reproduced the sketches shown in Figs. 4 through 8 of the celebrated [1863] treatise of Plateau and in photographs by Wang, et al. The same sort of phenomenon, bifurcation of rotating drops into non-axisymmetric shapes in qualitative agreement with theory, although the theory does not acknowledge the outer fluid, was reported by Wang, et al.

Acknowledgement

We wish to thank Robert Gulliver for his advice about how to solve the minimization problem. This work was supported by the National Science Foundation, Fluid Mechanics, and the U. S. Army, Mathematics. Computer results were obtained under a grant from the Academic Computing Services and Systems of the University of Minnesota.

This paper is dedicated to James Serrin for his 60th birthday.

References

Beer, A. Einleitung in die Matematische Theorie der Elastizität und Capillarität, A. Gresen Verlag, Leipzig, 1869.

Brown, R. A. and Scriven, L. E. “The shape and stability of rotating liquid drops”, Phil. Trans. Roy. Soc. London A297 (1980), 51-79.

Chandrasekhar, S. “The stability of a rotating liquid drop”, Proc. Roy.Soc. London A286 (1965), 1-26.

Guillopé, C., Joseph, D.D., Nguyen, K., and Rosso, F. J Mec. Théor. Appl. 6 (1987) 5.

Joseph, D. D. Stability of Fluid Motions II, Springer, 1976.

Joseph, D. D., Renardy, Y., Renardy, M. and Nguyen, K. “Stability of rigid motions and rollers in bicomponent flows of immiscible liquids”, J. Fluid Mech. 153 (1985), 151-165.

Joseph, D. D., Nguyen, K. and Beavers, G. S. “Non-uniqueness and stability of the configuration of flow of immiscible fluids with different viscosities”,J. Fluid Mech. 141 (1984), 319-345.

Joseph, D. D., Nguyen, K. and Beavers, G. S. “Rollers”, Phys. Fluids. 29 (1986), 2771.

Leslie, F. “Measurements of rotating bubble shapes in a low gravity environment”, J. Fluid Mech. 161 (1985), 269-280.

Moffatt, K. “Behaviour of a viscous film on the outer surface of a rotating cylinder”, J. Méc. 16 (1977), 651-673.

Plateau, J. A. F. “Experimental and theoretical researches on the figures of equilibrium of a rotating liquid mass withdrawn from the action of gravity”, Annual Report of the Board of Regents and Smithsonian Institution, Washington, DC, (1863) 270-285.

Preziosi, L. “Selected topics in the mechanics of two fluids and viscoelastic media”, Ph.D. Thesis. University of Minnesota, 1986.

Preziosi, L. and Joseph, D. D. “The run-off condition for coating and rimming flow”, J. Fluid Mech. 187 (1986) 99–113.

Princen, H. M., Zia, I. Y. Z. and Mason, S. G. “Measurements of interfacial tension from the shape of a rotating liquid drop”, J. Colloid Interface Sci. 23 (1967) 99-107.

Rayleigh, Lord. “The equilibrium of revolving liquid under capillary force”, Phil. Mag. 28 (1914) 161.

Rosenthal, D. K. “The shape and stability of a bubble at the axis of a rotating liquid”, J. Fluid Mech. 12 (1962) 358-366.

Ross, D. K. “The shape and energy of a revolving liquid mass held together by surface tension”, Austral. J. Physics. 21 (1968) 823-835.

Russo, M. J. and Steen, P. H. “Instability of rotund capillary bridges to general disturbances, experiment and theory”, J. Colloid Interface Sci. 113 (1986) 154-163.

Wang, T. G., Tagg, R., Cammack, L. and Croonquist, A. “Non-axisymmetric shapes of a rotating drop in an immiscible system” in Proc. 2nd Int. Colloq. on Drops and Bubbles, ed. by D. H. LeCroisette, NASA-JPL, 1981.

Yih, C. S. “Instability of a rotating liquid film with a free surface”, Proc. R. Soc. London A258 (1960) 63-86.

List of Figures

Figure 3 Schematic drawing of minimizing solutions. Minimizing solutions touch the axis with a perpendicular tangent. (a) Solutions of unduloid type are convex, 4≥J≥ –5.42285. (b) Solutions of nodoid type have a point of inflection –5.42285≥J≥ –8.18834. (c) Limiting (toroidal) form of the solution for J= –7.583908.

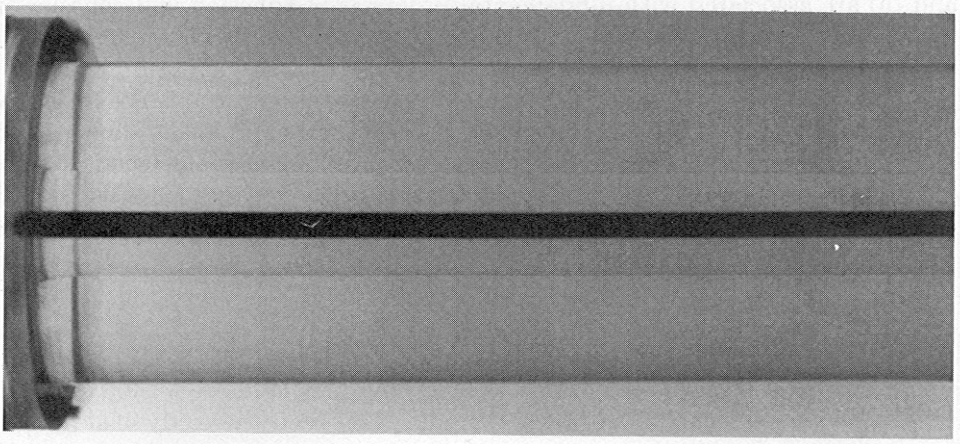

FIGURE 4. Cylindrical interface between 1000 cSt silicone oil and water when $J = 4.5$. The radius of rod is 0.24 cm.

Figure 4 Cylindrical interface between 1000 cs. silicone oil and water when J=4.5. The radius of the rod is 0.24 cm.

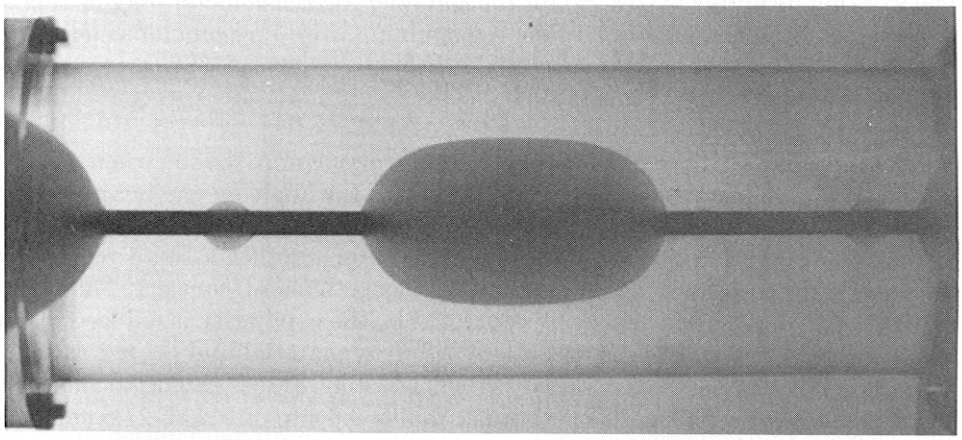

FIGURE 5. Array of bubbles of 95% silicone oil (12500 cSt) dyed with 5% castor oil ($\rho = 0.974$, $T = 20.5$) in water. $J = 1.87$ for the central bubble and 0.05 for the small ones. The radius of the aluminium rod is 0.24 cm.

Figure 5 Array of bubbles of 95% silicone oil (12500 cs.) dyed with 5% castor oil (□=.974, T=20.5) in water. The J for the central bubble is 1.87 and that for the small ones is 0.05. The radius of the aluminum rod is 0.24 cm.

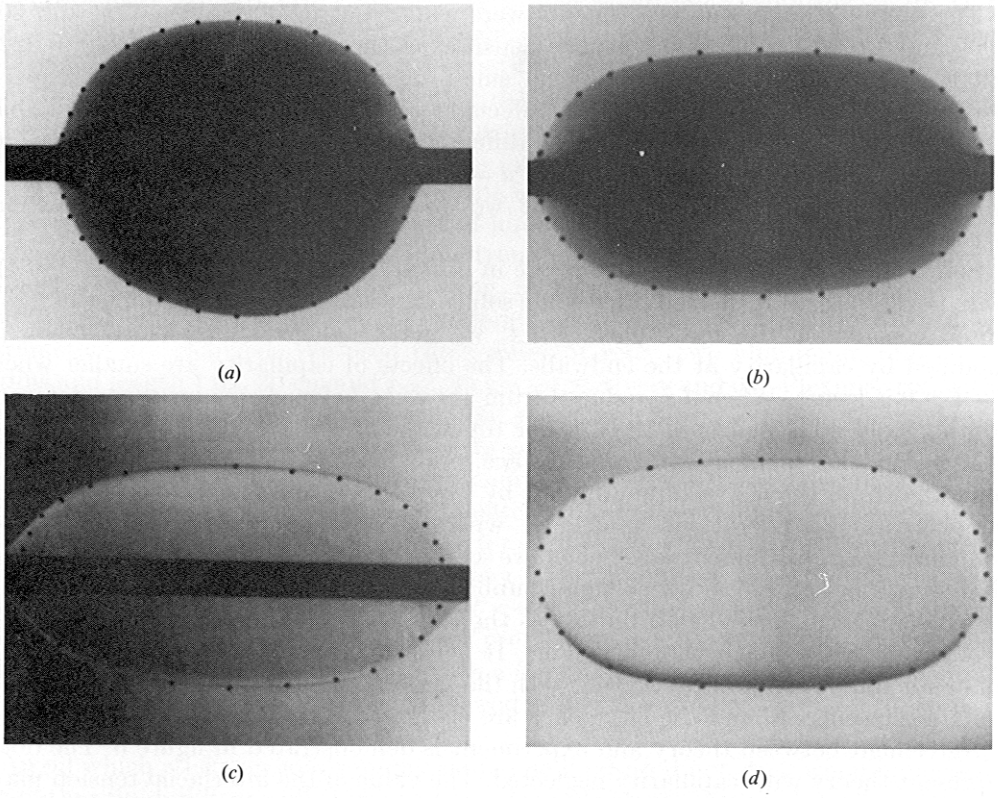

FIGURE 6. Numerical comparison. The dots are theory computed numerically (see (3.22)) neglecting the contact-line potential. The rod radius is 0.24 cm. (*a*) Bubble of 95% silicone oil (12500 cSt) dyed with 5% castor oil ($\rho = 0.974$, $T = 20.5$) in water when $J = 0.72$. (*b*) Bubble of 95% silicone oil (12500 cSt) dyed with 5% castor oil ($\rho = 0.974$, $T = 20.5$) in water when $J = 1.87$. (*c*) Bubble of silicone oil (1000 cSt, $\rho = 0.967$, $T = 22.1$) in water when $J = 2$. (*d*) Bubble of silicone oil (1000 cSt, $\rho = 0.967$, $T = 22.1$) in water when $J = 2$ without inner rod.

Figure 6 Numerical comparison. The dots are theory computed numerically (see (3.24)) neglecting the contact line potential. The rod radius is 0.24 cm.

a) bubble of 95% silicone oil (12500 cs) dyed with 5% castor oil (□=0.974, T=20.5) in water when J=0.72

b) bubble of 95% silicone oil (12500 cs) dyed with 5% castor oil (□=0.974, T=20.5) in water when J=1.87

c) bubble of silicone oil (1000 cs, □=0.967, T=22.1) in water when J=2

d) bubble of silicone oil (1000 cs, □=0.967, T=22.1) in water when J=2 without inner rod.

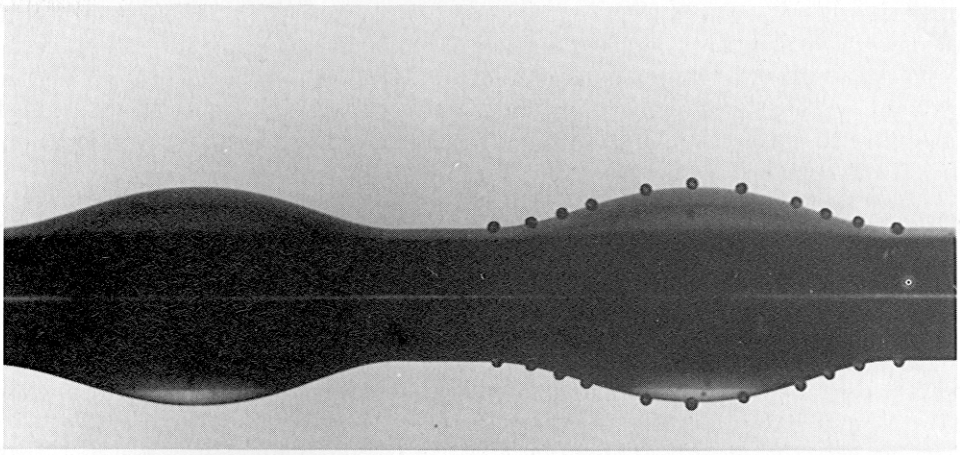

FIGURE 7. The rod is coated with STP and is rotating in air with $J = -0.95$, $a/d = 0.74$ and $Sh_0^2 = 0.57$. The dots compare the observed shape with the axisymmetric drop that has a tangent contact at $r = a$. The shape of this axisymmetric figure is determined by the method of §5.2.

Figure 7 The rod is coated with STP and is rotating in air with J= –0.95, a/d=0.74 and □=0.57. The dots compare the observed shape with the axisymmetric drop which has a tangent contact at r=a. The shape of this axisymmetric figure is determined by the method of Section 5.2.

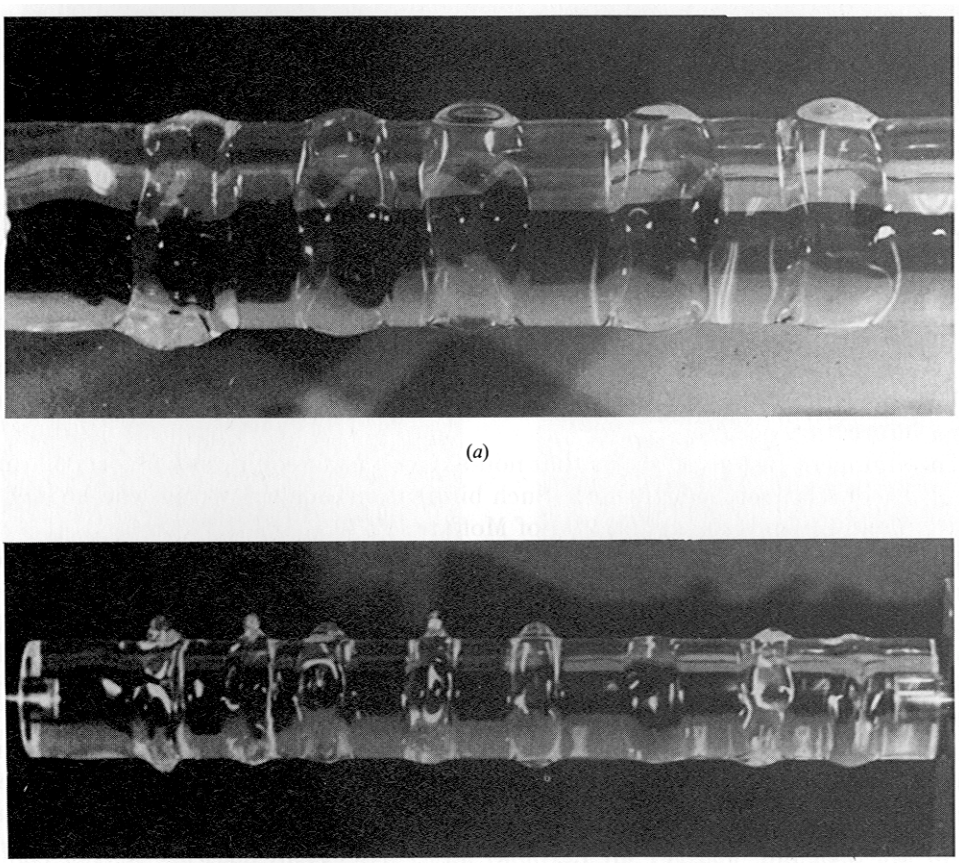

(*a*)

(*b*)

FIGURE 8. (*a*) Bifurcated non-axisymmetric solutions on rings of 6000 P silicone oil in air on a 2.04 cm rotating Plexiglas rod. (*b*) Instability of the bifurcated rings at a higher rotation rate.

Figure 8 (a) Bifurcated nonaxisymmetric solutions on rings of 6000 p silicone oil in air on a 2.04 cm rotating plexiglass rod. (b) Instability of the bifurcated rings at a higher rotation rate.

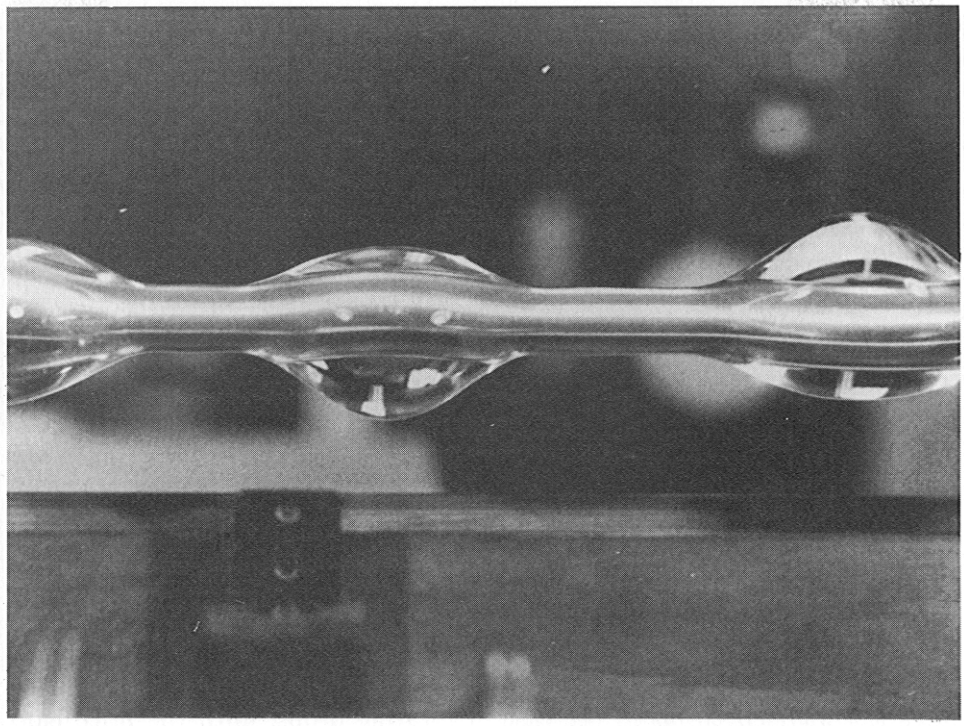

FIGURE 9. Silicone oil (6000 P) on a 1.02 cm radius aluminium rod rotating in air at 21.9 r.p.m. The lobes rotate much more slowly: left to right 15, 18.8 and 13.7 r.p.m. respectively.

Figure 9 Silicone oil (6000 p) on a 1.02 cm. radius aluminum rod rotating in air at 21.9 rpm. The lobes rotate much more slowly, left to right, 15, 18.8 and 13.7 rpm, respectively.

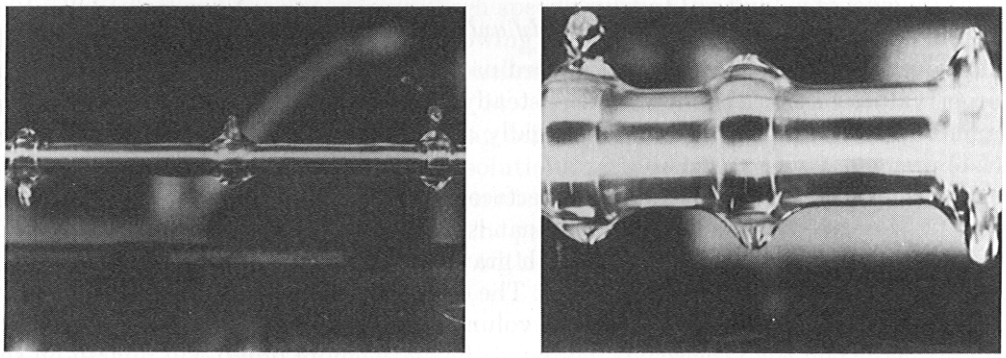

(*a*) (*b*)

FIGURE 10. The 6000 P silicone oil is thrown off radially. The effects of gravity are negligible. The configuration is nearly steady in a rotating coordinate system. (*a*) $\Omega = 99.15$ r.p.m., $a = 1.02$ cm; (*b*) $\Omega = 31.76$ r.p.m., $a = 2.04$ cm. The surface velocities of the three rings (*b*) from the left to right are 31.41, 31.57 and 31.53 r.p.m. respectively.

Figure 10 The 6000 p silicone oil is thrown off radially. The effects of gravity are negligible. The configuration is nearly steady in a rotating coordinate system.

a) □=99.15 rpm, a=1.02 cm

b) □=31.76 rpm, a=2.04 cm

The surface velocities of the three rings (b) from left to right are 31.41, 31.57 and 31.53 rpm respectively.

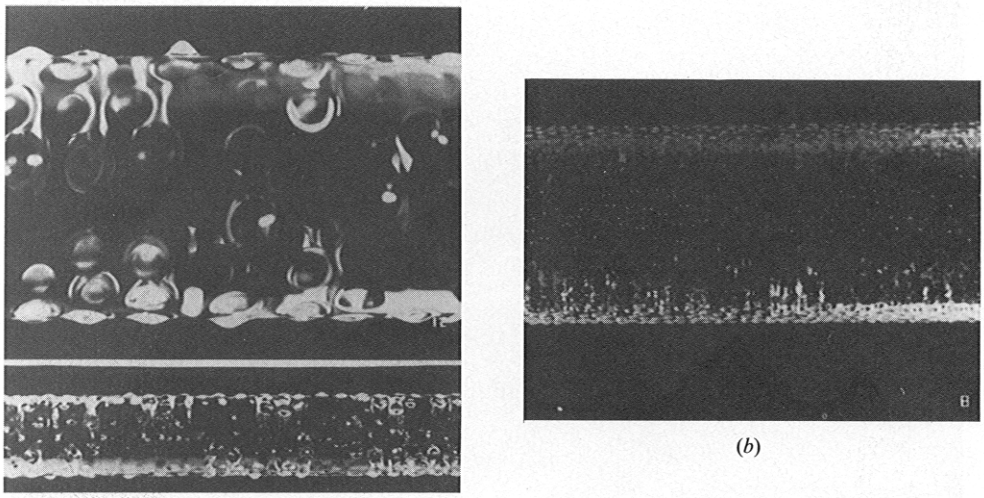

(*a*) (*b*)

FIGURE 11. Pendant drops of 6000 P silicone oil in air on a rod of radius 2.04 cm. The motion is perfectly steady in a rotating coordinate system. Gravity is negligible. (*a*) $\Omega = 500$ r.p.m. (*b*) 1000 r.p.m.

Figure 11 Pendant drops of 6000 p silicone oil in air on a rod of radius 2.04 cm. The motion is perfectly steady in a rotating coordinate system. Gravity is negligible.

a) □=500 rpm

b) □=1000 rpm

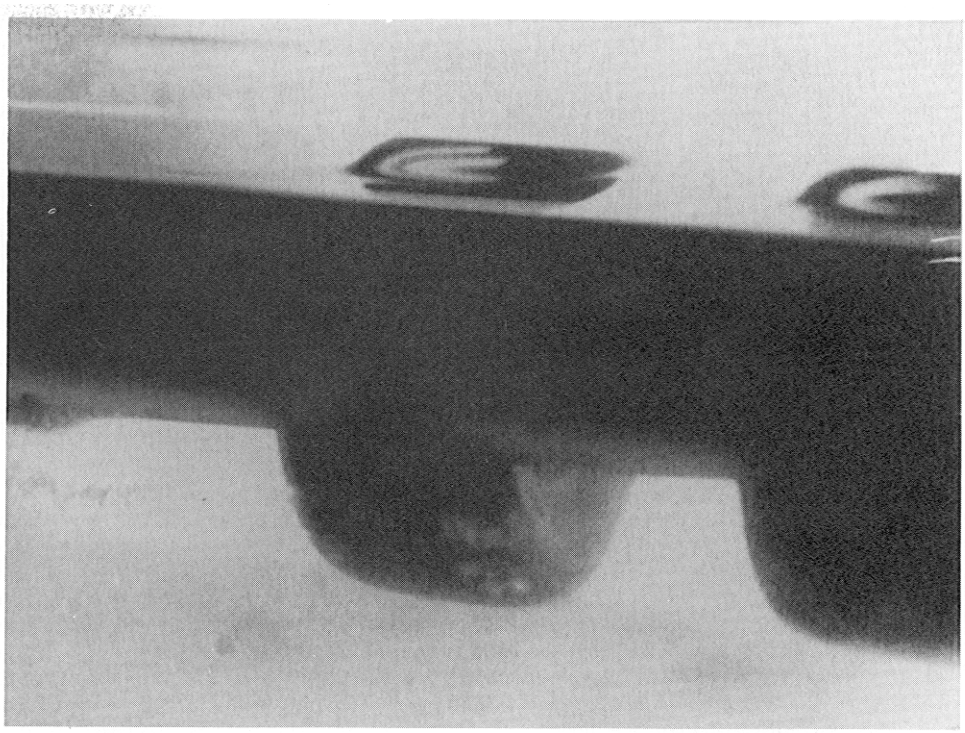

FIGURE 12. STP roller immersed in water, lubricated by water everywhere, poking its head into air. The shape of this roller is nodoid like (see figure 3).

Figure 12 STP roller immersed in water, lubricated by water everywhere, poking its head into air. The shape of this roller is nodoid (see Fig. 3).

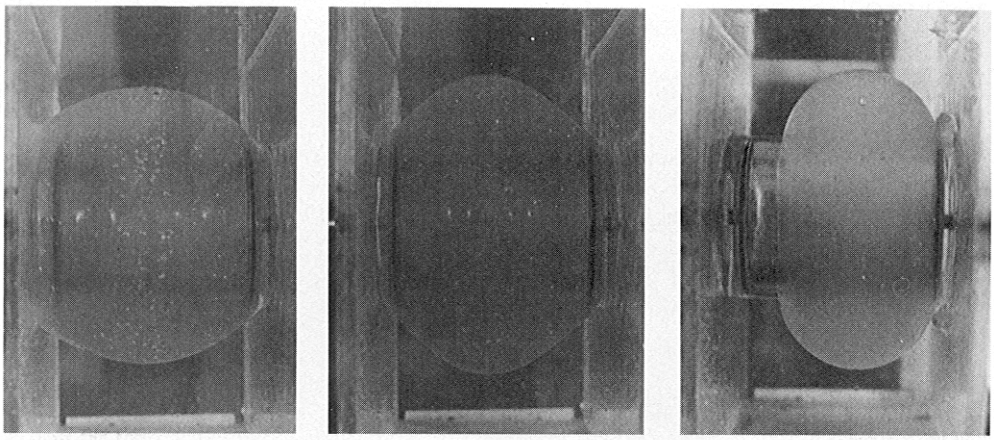

(a) (b) (c)

FIGURE 13. Detachment of rollers from the sidewalls. The diameter and length of the Plexiglas cylinder are 5.7 cm and 10.8 cm respectively. The roller of silicone oil (1000 P, $\rho = 0.997$) rotates in water. (*a*) $\Omega = 0.75$ rad/s. The roller is attached to the sidewalls. (*b*) $\Omega = 1.19$ rad/s. The speed is increased. The wavelength of the roller decreases as in a rotating drop and the roller detaches from the wall. The critical Ω for detachment is 1.14 rad/s. (*c*) $\Omega = 1.19$ rad/s, but three days later, the minimizing solution appears to have the form required for a rotating drop. In fact, we get qualitative agreement between the theory given in §6.2 and the experiments if we imagine the roller to be a drop of density ρ (water) $- \rho$ (oil) > 0. We call attention to the change in the contact angle with the position of the contact line.

Figure 13 Detachment of rollers from the side walls. The diameter and length of the plexiglass cylinder is 5.7 cm. and 10.8 cm., respectively. The roller of silicone oil (1000 p, □=0.997) rotates in water.

(a) □=0.75 rad/sec. The roller is attached to the side walls.

(b) □=1.19 rad/sec. The speed is increased. The wave length of the roller decreases as in a rotating drop and the roller detaches from the wall. The critical □ for detachment is 1.14 rad/sec.

(c) □=1.19 rad/sec., but three days later, the minimizing solution appears to have the form required for a rotating drop.

In fact, we get qualitative agreement between the theory given in Section 6.2 and the experiments if we imagine the roller to be a drop of density □(water) – □(oil) >0. We call attention to the change in the contact angle with the position of the contact line.

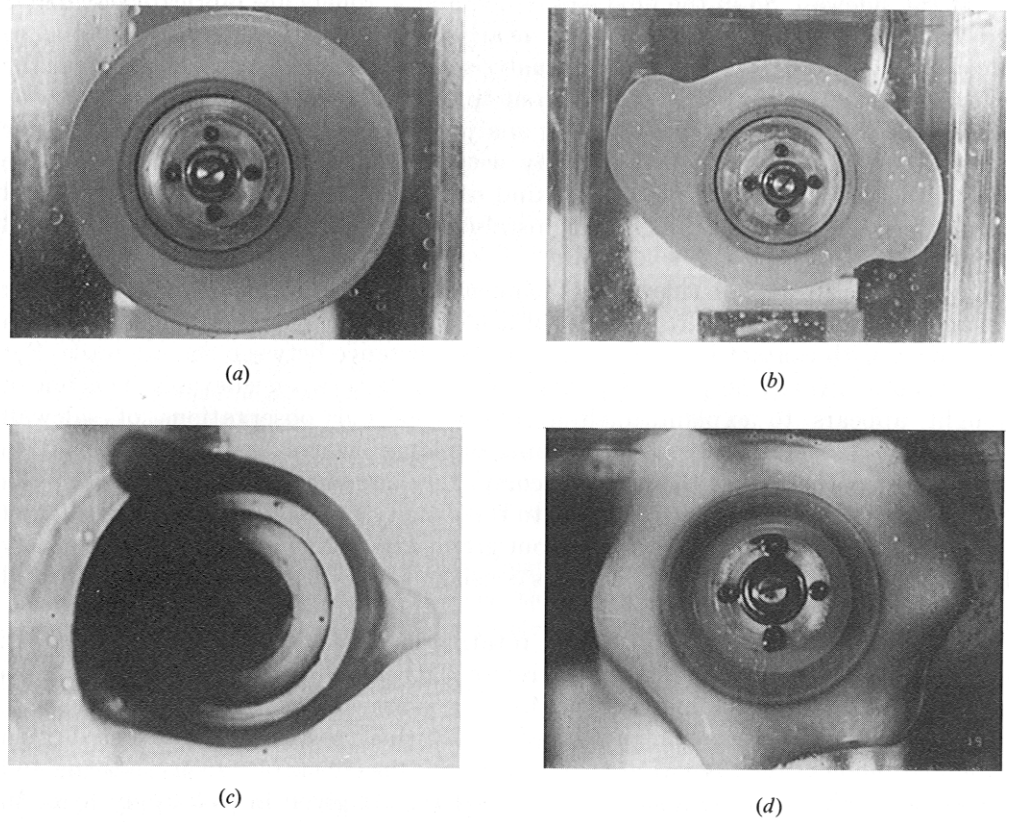

(*a*) (*b*) (*c*) (*d*)

FIGURE 14. Bifurcated configurations of silicone oil in water. Only the one-lobed figure is stable in our experiments; the other figures eventually degenerate into a single lobe. This is consistent with predictions given by Brown & Scriven (1980) for a related problem. The one- and two-lobed structures resemble figures 4 and 8 sketched in the work of Plateau (1863). (*a*) One lobe, $\Omega = 0.47$ rad/s; (*b*) two lobes, $\Omega = 0.83$ rad/s; (*c*) three lobes, $\Omega = 1.49$ rad/s; (*d*) six lobes, $\Omega = 3.18$ rad/s.

Figure 14 Bifurcated configurations of silicone oil in water. Only the one-lobed figure is stable in our experiments; the other figures eventually degenerate into a single lobe. This is consistent with predictions given by Brown and Scriven [1980] for a related problem. The one- and two-lobed figures resemble Figures 4 and 8 sketched in the work of Plateau (1863).

(a) One lobe, □=0.47 rad/sec

(b) Two lobes, □=0.83 rad/sec

(c) Three lobes, □=1.49 rad/sec

(d) Six lobes, □=3.18 rad/sec